Journal of Harbin Engineering University Vol 44 No. 7

ISSN: 1006-7043 July 2023

An Advanced Lcl-Dlnn Algorithm Based Retinal Disease Detection Using Retinal Fundus Image

Sheeja Mary F
Research Scholar
Dept. of Computer Science and Engineering
Annamalai University
Annamalainagar - 608002
Email: zsheeja@yahoo.co.in
Dr. V. Asanambigai
Assistant Professor
Dept. of Computer Science and Engineering
Annamalai University
Annamalainagar – 608 002
Email: tradingbaskeran@gmail.com
Dr. A. Lenin Fred
Principal
Mar Ephraem College of Engineering and Technology
Marthandam
Email: leninfred.a@gmail.com

ABSTRACT

Medical image processing has recently increased the precision with which medical images are used to identify disorders in people. Using Deep Learning (DL) methodologies, which allow automatic learning of the associated characteristics for specific tasks rather than handmade procedures, has significantly improved the analysis of medical images. Currently, a variety of methods for autonomously segmenting retinal fundus images have been developed. However, to increase computational complexity and decreased efficiency, they were unable to provide superior accuracy. In this study, Learning Curved Layered Deep Learning Neural Network (LCL-DLNN) is used to suggest an effective detection method employing retinal fundus images. The retinal images are first pre-processed in two processes, such as image cropping and image contrast level, to improve the image quality. Second, to increase the input image quality from segmented images and increase prediction accuracy, we design the Edge Stop Functional Iterative Region Growing (ESFIRG) method. Finally, the retinal fundus image can be used to forecast whether or not the proposed LCL-DLNN approach would perform. The suggested method is implemented on the MATLAB platform, and performance is assessed using presentation metrics. The suggested technique outperforms the currently used research approaches in experimental analysis.

Keywords - Learning Curved Layered Deep Learning Neural Network (LCL-DLNN), retinal fundus image, retinal disease, Edge Stop Functional Iterative Region Growing (ESFIRG), segmentation and prediction.

I. INTRODUCTION

Recent years have seen a significant transformation in clinical imaging, notably with the introduction of cutting-edge imaging devices and modalities. Due to their enormous potential for the early diagnosis of medical disorders, clinical imaging has drawn the attention of a broad spectrum of research interests. Early identification aids in accurate diagnosis and therapy, which almost completely eradicates the medical problem [1][2]. The ability to diagnose numerous symptoms and illnesses using the same imaging modality is an intriguing aspect of clinical imaging. For instance, retinal imaging may be used to identify cataracts, blurriness in the eyes, etc. Additionally, it serves as a critical marker for several blood-related diseases as diabetes and hypertension [3]. Thus, owing to late detections and segmentations, the function

of medical imaging has become more important in practically all healthcare sectors, dramatically lowering the death rate. Thus, eye screening together with prompt diagnosis and care is a widely accepted approach to prevent vision loss and harm to other body parts. Visual impairment might be prevented by early segmentation and diagnosis of ocular illnesses in the early stages of disease development [4][5].

Aspects of current retinal illness diagnosis that are crucial include automated segmentation of retinal fundus images, localization and detection of the optic disc and blood vessels, and identification of the macula, exudates, and haemorrhage [6]. It is possible to screen for and diagnose a number of diseases, including hypertension, atherosclerosis, glaucoma, retinopathy, diabetes, prematurity, and Age-related Macular Degeneration(AMD), by identifying retinal blood vessels and extracting their characteristics, such as length, width, angle, colour, and tortuosity [7][8]. Segmenting the blood vessels in eye images is also necessary for biometric identification, computer-assisted surgery, and multimodal image registration. It takes a lot of time and effort to manually separate the blood vessels in retinal images [9]. For the creation of decision support systems for the early diagnosis and treatment of visual diseases, the segmentation of the retinal vasculature is thought to be crucial [10].

An extensive quantity of fundus images from retinal screening programs have been analyzed using Machine Learning (ML) algorithms in several prior research to concentrate on the automated identification of retinal disorders [11]. Automated retinal illness identification was carried out using a variety of machine learning methods, including the K-nearest neighbour algorithm, the Naive Bayes classifier, the Artificial Neural Network (ANN), and the Support Vector Machine (SVM). While the majority of research focused on diagnosing Diabetic Macular Retinopathy (DMR), only a small number of studies produced machine learning models for AMD identification. The area of machine learning technology saw the emergence of Deep Learning (DL) for the analysis of medical images.

Numerous papers have used ANN models to differentiate between glaucoma and non-glaucoma [12]. A glaucoma research team has reported the use of visual field analysis and deep feedback neural networks to find preperimetric glaucoma. Nuclear cataract severity was graded using an automated deep Convolutional Neural Network (CNN) [13][14]. Additionally, a comparable method for diagnosing retinopathy of prematurity utilizing photographs of newborns' retinas was created. Recent findings from Abramoff's research team show that this learning method outperformed earlier algorithms in terms of automated DMR detection [15]. The key area of interest in this research work is the aforementioned topic of retinal imaging for the diagnosis of illnesses connected to the retina of the eye. Retinal image processing for early disease identification is a difficult undertaking with several limitations on how to separate the retina from the background.

Problem Statement

The current study approaches have a few issues that are mentioned below:

- ❖ Less method for detecting eye illness are accessible when using a deep learning model.
- ❖ A number of strategies made use of a tiny database of retinal images. When used for databases of huge sizes, the effectiveness of present solutions is in doubt.
- ❖ The process for identifying retinal disorders still has accuracy issues.

To solve those problems of the existing research works this paper proposed efficient retinal disease detection. The contribution of the research work is described as follows,

- To accurately detect the retinal disease using Learning Curved Layered Deep Learning Neural Network (LCL-DLNN).
- Advanced approach deep learning approach is used.
- To segment each function of the retinal image using ESFIRG.

The framework of the study that is being given is set up as follows: in section 2, it is described

about previous research has been done on medical image analysis. The proposed portion is described in section 3. The experimental investigation of the suggested study is completed in section 4. The study is ended with potential improvements in section 5.

II. RELATED WORK

Medical image analysis technology has evolved mainly to deep learning algorithms. However, DL usage for retinal issues is a very recent development. DME, drusen, and CNV are just a few of the several eye disorders that may be seen and evaluated using OCT scans of the human eye.

Butt *et al*. [16] have presented a method based on in-depth image analysis to diagnose glaucoma and found that the retinal fundus was the location of glaucoma. In order to give thorough image analysis, these attributes are integrated with the majority of the retrievable information, such as cup/disc, inferior, superior, nasal, and temporal ratios. The suggested model is used to portray the retinal fundus images, which aids the ophthalmologist in making more informed decisions about the care of the human eye.

The Deep Neuro Fuzzy Network (DNFN)-based technique can be used to diagnose glaucoma created by Gampala *et al*. [17]. The retinal images serve as the primary input for the noise reduction procedure. The Optical Disc (OD) is then found using either the fuzzy black hole entropy clustering method or the deep learning model. DNFN is learning to track blood vessel OD and delivery with the new MultiVerse Rider Wave Optimisation (MVRWO). The new MVRWO combines the water wave optimisation, the multiverse optimizer, and the rider optimisation method.

The investigation of early detection of age-related eye illnesses was conducted by Muthukannan *et al*. [18]. The pre-processed images were put into a CNN that had been altered using a Flower Pollination Optimisation Algorithm (FPOA) method for feature extraction. Hyper parameters were tweaked using FPOA to train CNN. As a result, the network's accuracy and effectiveness have increased. From the CNN output, a Multiclass Support Vector Machine (MSVM) classifier was used to ascertain the kind of sickness.

Ramya *et al* [19] have implemented a classification of exudates from the fundus images showed how the binary local search optimizer based on a hybrid CNN can be optimised using a particle swarm technique. Using the method outlined in this work, the fundus image is maintained in its whole while being expanded to the required size. The CNN anticipation is then given an input feature vector created by extracting features from zoomed background photos. Exudates from fundus images now come in a wide variety. To adjust hyper parameters and lessen computational complexity, Particle Swarm Optimisation (PSO) and Binary Local Search Optimizer (BLSO) are also utilised.

Kadry *et al* [20] developed an automated approach to identify Age-related Macular Degeneration (AMD) utilising a Deep Learning (DL) algorithm with hand-crafted deep features and series-chaining. The following research steps are now extracting features: initial data processing, deep feature extraction using VGG16, manual feature extraction, selection of optimal features with Mayfly algorithm, serial feature chaining, binary classification, and validation. The Local Binary Model (LBP), Pyramid Histogram of Oriented Gradients (PHOG), and Discrete Wavelet Transform (DWT), which are built manually from the test images, are then merged with the deep features of VGG16. The effectiveness of the novel strategy to be separately assessed using Optical Coherence Tomography (OCT) and Retinal Fundus Imaging (RFI).

Singh *et al.,*[21] have presented two layered techniques (BA-BCS, BCS-PSO) combining the Bat Algorithm (BA), Binary Cuckoo Search (BCS), and Particle Swarm Optimisation (PSO) are applied. Additionally, we separately examined BA, BCS, and PSO's performance. Three machine learning classifiers may be equipped with these five (one- and two-tier) approaches to provide the most precise subsets with the least amount of functionality.

Khaing *et al*. [22] investigated a completely automated hybrid approach for OD localisation. On retinal images captured with mobiles and pocket cameras, it has been tested. It was created for retinal images. If an image includes full vasculature, the HLM locates OD sites using the exclusion technique; if not, it employs a newly developed line identification method. The circle fitting technique is used by the HLM after an active contour model has been used for OD segmentation.

III. PROPOSED AN EFFICIENT RETINAL DISEASE DETECTION USINGRETINAL FUNDUS IMAGE

In the modern world, learning models based on Artificial Intelligence (AI) are often utilised in several applications for medical image interpretation. The implementation of the in-depth research is done to find solutions to issues like categorising different kinds of medical photographs and identifying diseases. In order to diagnose the effects of diabetes on the eye and prevent early blindness, the identification of eye illness is of utmost importance. For the purpose of detecting eye illness, several models were put into practise. But still some research drawbacks are presented to solve that problem this research methodology proposed Advanced Neural Network (ANN) based eye disease detection system. The proposed methodology consists of four phases that are pre-processing by ADPHE, segmentation by using ESFIRG, feature extraction and feature classification by using LCL-DLNN. Figure 1 displays the block diagram for the suggested research technique.

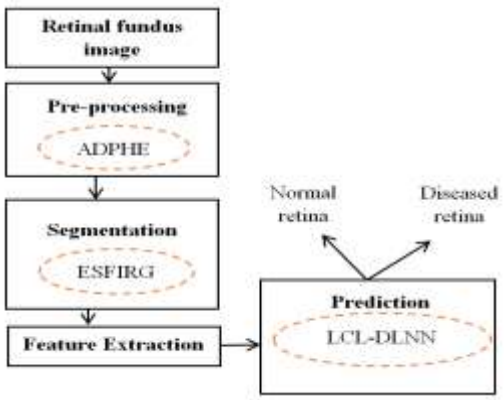

Figure 1 Block diagram for the proposed methodology

3.1 Pre-processing

The supplied image is pre-processed in this stage. First, the input image is cropped, and then the Double Plateau Histogram Equalization (DPHE) technique is used to increase the image contrast level. An image with a higher contrast level contains more details about the texture of the disc, blood vessel, etc. However, adding noise to the input images during improvement is possible. This study approach sets the limit based on an average estimate of the intensity of the images pixels to address that issue. Averaged Double Plateau Histogram Equalization (ADPHE) is the name specified to the suggested research approach. To boost the enhancement quality, the suggested ADPHE has been applied independently to the foreground and background regions. To reduce the saturation impact and control the rate of amplification in both regions, two plateau thresholds are used. The lower threshold is designed to avoid merging while maintaining the details with less pixels, while the higher threshold is utilised to prevent over-enhancement [23]. Equations (1) and (2) provide $L_P(x)$ and $U_P(x)$ display the Probability Density Function (PDF) computed by ADPHE in the background and foreground, respectively. LU_T, LL_T are the image's upper and lower thresholds for the background area and UU_T, UL_T as well as foreground portion of the image's upper and lower thresholds.

$$L_P(x)=\begin{cases} LU_T, \text{ if } L_P(x) > LU_T \\ L_P(x), \text{ if } \ LL_T < L_P(x) \le LU_T \\ LL_T, \text{ if } \ 0 \le L_P(x) \le LL_T \end{cases} \quad (1)$$

$$U_P(x)=\begin{cases} UU_T, \text{ if } U_P(x) > UU_T \\ U_P(x), \text{ if } \ UL_T < U_P(x) \le UU_T \\ UL_T, \text{ if } \ 0 \le U_P(x) \le UL_T \end{cases} \quad (2)$$

The values of LL_T, LU_T, UL_T *and* UU_T are chosen from 0 to 0.0001, 0.0001 to mean L_P, L_P mean to U_P mean, and U_P mean to 1 correspondingly. Here, a shared exponentiation parameter (μ) that affects both the foreground and background is added. Maintaining homogeneity between the two zones is the major goal of utilizing this parameter. Background image's weighted function is shown in Equation (3),

$$Lw_{pd}(n) = MaxF_0(L_p) * \left(\frac{L_p(n) - MinF_0(L_p)}{MaxF_0(L_p) - MinF_0(L_p)} \right)^{\mu} \quad (3)$$

For the foreground image, the weighted function is shown in Equation (4),

$$Uw_{pd}(n) = MaxF_0(U_p) * \left(\frac{U_p(n) - MinF_0(U_p)}{MaxF_0(U_p) - MinF_0(U_p)} \right)^{\mu+\eta} \quad (4)$$

The average adjustable parameters are μ and η for exponentiation. These parameters' ideal values are chosen from a range of 0 to 0.5 and 0.5 to 1, respectively.

3.2 Segmentation

After the quality of the image supplied is upgraded, the segmentation technique is used to separate the enhanced image into several components, such as the optic disc, optic cup, and optic nerve. This research methodology proposed an Edge Stop Functional Iterative Region Growing (ESFIRG) algorithm. This research methodology proposed an Edge stopping function in the energy calculation to take the weak edge boundary into account as well [24]. The iteration region growing approach, also known as the snake contour model, offers better segmentation results. The real input fundus image for the study approach is in the form of low-intensity fake areas. The denoising process includes transforming the image into a domain, where the threshold improves simple noise identification. The denoise is rebuilt using the inverted change. Therefore, edge stop functional denoising is required to remove the erroneous areas from the image while maintaining the vessel edges.

A region is an independent geographic grouping of pixels that is represented by a node in a Region Growing Adjacency Graph (RGAG), and a link is the shared border between two regions. The segmentation and classification algorithms leverage the edge strength between each pair of neighbouring regions. It has been shown in Equation (5) that it is feasible to penalize weak edges more severely than strong edges instead of equally for all boundary-site pairings.

$$\omega(\nabla_{st}) = \omega(|c_s - c_t|) = e^{-\left(\frac{|c_s - c_t|}{D}\right)^2} \quad (5)$$

Where γ is a positive integer and s and t are the nearby spots that form a pair-location clique. Each pixel's gray level is constant c_s and tied to its matching class name m_s. The ESFIRG technique approaches the segmentation formulation of (5) from the common Gaussian mixture issue using a series of objective functions in (6) (with D rising).

$$\Re = \arg\min_{\{n_s, s\in S\}} \left\{ \sum_{s\in S} \left(\frac{1}{2}\ln\left(2\pi\tau_{n_s}^2\right) + \frac{\left(c_s - \mu_{n_s}\right)^2}{2\mu_{n_s}^2} \right) + \gamma \sum_{\langle s,t\rangle \in Z} \left[(1 - \beta(c_s - c_t))\omega(\nabla_{st}) \right] \right\} \quad (6)$$

Iterative segmentation is used in the IRG procedure. At each iteration, a region-merging technique is used to solve the objective function (6) for a particular D, with region-based labelling [25] serving as the merging criterion.

$$\beta E = \sum_{s\in\eta_x} \ln(\omega_x) - \sum_{s\in\eta_y} \ln(\omega_y) - \sum_{s\in\eta_z} \ln(\omega_z) - \gamma \sum_{\substack{s\in\partial\eta \\ t\in\partial\eta_z, t\in\delta_s}} \omega(|c_t - c_s|) \quad (7)$$

Where η_x and η_y are the names of the two regions, $\eta_z = \eta_x \bigcup \eta_y$ and $\partial\eta_x$ is the collection of border locations of η_x (i.e. $\exists t \in \delta_s, m_s \neq m_t$). If βE generates a undesirable, η_x and η_y can

be added together; βE if produces a positive value but η_x and η_y cannot be added together. After the region-merging process is complete (i.e., no more region pairs satisfy the merging requirement), an RGAG may be updated using the recovered regions. Using an edge stop functional based on the RGAG, we mimic the region-based labelling procedure and the associated single-node clique-energy function.

$$\Delta_1(m_x)=\sum_{s\in\eta_t}\left\{\frac{1}{2}\ln\left(2\pi\mu_{m_t}^2\right)+\frac{\left(c_s-\tau_{m_t}\right)^2}{2\mu_{m_t}^2}\right\} \tag{8}$$

as well as the pair-node clique energy being

$$\Delta_2\left(m_x,m_y\right)=\begin{cases}\gamma\sum\limits_{\substack{s\in\partial\eta\\ t\in\partial\eta_z,t\in\delta_s}}\omega\left(\left|c_t-c_s\right|\right), & if\ \ c_x\neq c_y\\ 0\end{cases} \tag{9}$$

Where, τ_{m_t} and $\mu_{m_t}^2$ denotes the mean and variance of all the pixel values from Equation (9) in the class are and the label of the area is m_s, m_i. The global minimum of the sum of the aforementioned energies throughout the whole RGAG, which is exactly given in Equation (6), may be used to produce a label for the current iteration.

Algorithm: The pseudocode for the proposed ESFIRG

1. Create a baseline RGAG and give each node a random class label. At initially, D=0;

2. Calculate the Gaussian feature model parameters for each class using the segmentation solution currently in use that corresponds to the RG nodes and the class labels.

3. Find the minimal energy $\beta E_{\min}$ difference between each pair of association nodes that has the same area name by computing the energy difference βE according to equation (8).

4. If $\beta E_{\min}$ is negative, combine the two nodes that correspond to it to create one new node, then return to step 3. If not, go on to step 5.

5. Identify the new RGAG by labelling it. The procedure randomly scans each node, selecting the label for each scanned node that yields the lowest amount of energy for equation (7).

6. If the maximum number of iterations has not been reached, Increase D and return to step 2

3.3 Feature Extraction

The segmented retinal image is used in this stage to extract characteristics. The optic disc and/or cup's diameter, the optic nerve's length, and the thickness of the optic nerve may all be employed as characteristics of the retinal image. Here, using Gray-Level Co-occurrence Matrix (GLCM) approach, which is one of the most considerable characteristics of an image texture descriptors from the blurred retinal images. This can be attained by looking at the dimensionality of the gray levels in the area. The attributes of each pixel value as well as those of its neighborhood are included in the texture feature. The gray-level co-occurrence matrix seems to be a popular statistical technique for feature extraction. In GLCM, a matrix shows how a pair of pixels' (x,y)values change in accordance to an image's spatial connection. These pixels together make up a feature vector that indicates whether a pixel belongs to tissue or blood vessels [26]. Angle $(\cdot)$and displacement (d)between x and y establish the spatial connection. The entire number of gray levels in an image is represented by the width and height of the GLCM matrix. For each retinal image, a total of 22 characteristics are recovered after constructing a gray-level co occurrence matrix. The extracted GLCM -like images for a retinal image of drive is shown in Figure 2.

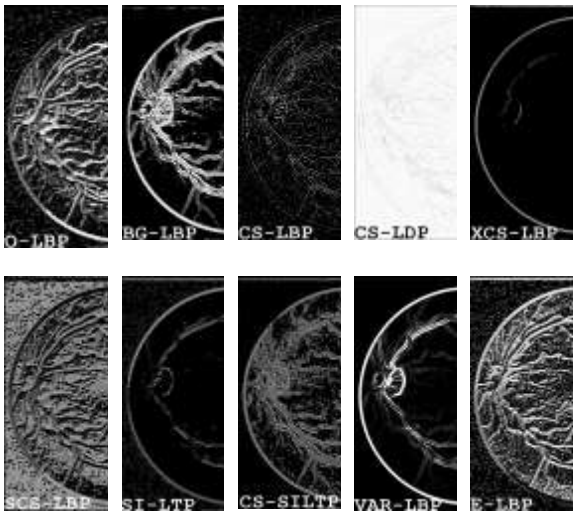

Figure 2 The extracted GLCM -like images for a retinal image of DRIVE

3.4 Prediction

For the detection of retinal disease this research methodology proposed a Learning Curved Layered Deep Learning Neural Network (LCL-DLNN). The deep learning neural network provides better outcome because it deeply learns the inputs. The problem of the deep learning approach is generalization error problem which creates the over fitting problem. In order to solve those problems this research methodology considers the learning curved layer based on the layer the weight and bias values are updated for the current learning process. Thus, the classifier predicts the image is normal retinal image or disease effected retinal image. Deep learning algorithms are capable of discovering many patterns and useful characteristics on their own from unprocessed data. CNN is a well-known deep learning architecture for image processing that is often used in the identification of retinal diseases.

A. Input layer

A collection of input images is stored in the input layer as an array of integers that only contains the pixels of the image. Images are transformed into a matrix array using calculations depending on the image's size and pixel count.

B. Convolution layer

Extrapolating recognizable features from the input image is the responsibility of the convolution layer. The input matrix is transformed into tiny, typically sized 3×3 sets of reduced matrix that are known as filters. A tensor of feature maps is created by applying the filters to every aspect of the input matrix in the convolution layer. Convoluting the input matrix is primarily done to reduce the number of weights that must be learned—both the set of high-level features and the set of low-level information, such as colors, orientation, edges, and padding. Depending on the characteristics to be retrieved, the number of convolution layers may be increased [27]. The lowest layer is used to extract low-level features, while the top layer is used to extract a wide variety of characteristics. More functionality may be extracted as the layer count rises. The input image is convolutional when applying 2D digital filters. Each pixel's value is altered as a consequence of this process, which relies on nearby pixels. As a result, the image transforms from a pixel-by-pixel representation to a feature map. Each point on the feature map that was created may be assessed as in Equation (10):

$$N_{Px} = \sum_{k\in S} \alpha_k * \beta_k \tag{10}$$

N_{Px}, represents the new value of a preset pixel and α_k while the old adjacent pixels are multiplied by the filter components β_k .

C. Pooling layer

The grouping layer reduces the size of the images. To create a value, the adjacent image pixels are concatenated into a deterministic component. Retaining the highest or typical pixel value the suggested framework calls for the most possible pooling. A maximum pooling example is shown in Figure 3.

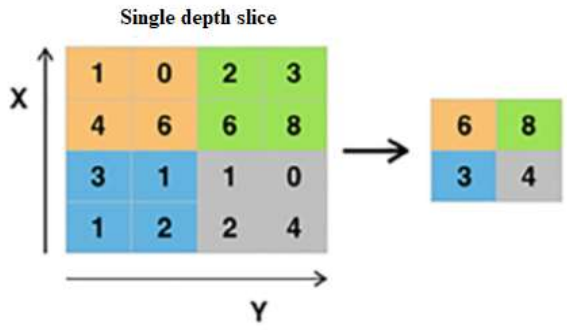

Figure 3 Maximum pooling layer

D. Fully-Connected (FC) layer

The class dimensions at the FC layer are tightly packed with the input data dimensions. During learning curve layer training, bias settings for the present learning process are modified, and outputs from the clustering layer are gathered with various weights. This is then given to the FC layer. The LCL technique involves using a number of parametric model families $\{F_1, F_2, ..., F_x\}$ to simulate the partly observed learning curve $\delta_{c:n}$. A collection of parameters is used to characterize each of these parametric functions F_x. We may use each to predict performance at time step T as $\delta_T = F_x(T|\theta) + \varepsilon$ long as we assume additive Gaussian noise $\in \sim \Omega(0, \sigma^2)$; the probability of a single observation under the δ_T model F_x is therefore given in Equation (11),

$$p(\delta_T|\theta_x, \sigma^2) = \Omega(\delta_T; F_x(T|\theta_x), \sigma^2) \quad (11)$$

Here, we choose from a huge collection of learning curves using parametric curves. We merge all models into a single, more powerful X model rather than choosing one at a time. A weighted linear combination provides this combined model:

$$F_{Comb}(T + \varepsilon) = \sum_{x=1}^{X} wt_x F_x(T|\theta_x) \quad (12)$$

From Equation (12), the new vector of integrated parameters,

$$\varepsilon = [wt_1, ...wt_x, \theta_1, ..., \theta_x, \sigma^2] \quad (13)$$

Equation (13), contains a weight wt_x for each model, each model's specific parameters θ_x, and σ^2 the noise variance $\delta_T = F_{comb}(T|\varepsilon) + \varepsilon$. It determines the likelihood that the feature maps belong to a certain class by taking features from all previous layers, combining them into a single vector, as shown in Figure 4 below. To achieve the most accurate weights, this layer provides back propagation and may iterate to the network's earlier levels.

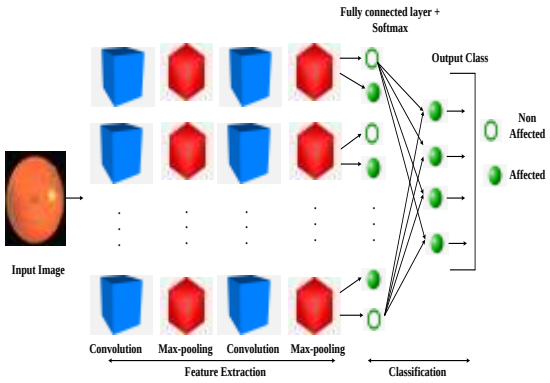

Figure 4 Structure of the proposed LCL-DLNN

D. Classification layer

The most recent CNN scale is used to categorise the FC level output. In this layer of the recommended design, the selection of the classification procedure is made using the Soft-max activation function.

E. Soft-max function

The CNN's activation functions are regarded as a crucial component. The activation function's objective is to introduce nonlinearity into the neuron output [28]. The suggested framework makes use of the soft-max function to make decisions. It is a straight forward kind of activation. Between 0 and 1 is the output range. It is used for multi-class and binary classification.

$$\rho(G_i) = \frac{e^{G_i}}{\sum_{i=1}^{j} e^{G_i}} \quad (14)$$

The G is regarded as the classification layer's input from Equation (14), and i is an index of the output $i = 1,\ldots..,\ldots.. j$ .In the further section the performance of the proposed research methodology is analysed.

IV. RESULTS AND DISCUSSION

Here, the performance of the proposed method detects the retinal disease using LCL-DLNN is analyzed with the existing research methodology such as Deep Belief Networks (DBN), Convolutional Neural Network (CNN) and Recurrent Neural Network (RNN) technique. The proposed research methodology is implemented in the working platform of MATLAB.

4.1 Description of Dataset

The dataset for diabetic retinopathy was chosen from the Kaggle website. 3662 retinal images from 5 categories—No_DR, Mild, Moderate, Severe, and Proliferative—make up the dataset. The photos are 224 × 224 pixel scaled scan images with a Gaussian filter. The training model is first generated when the dataset has been placed onto the local storage. 20% of the photos are utilized for validation, while the remaining 80% are used for training [29]. 2930 of the 3662 total photos were selected for training purposes. Rescaling settings are used to normalize images.

4.2 Performance Metrics

In this part, the proposed LCL-DLNN-based route selection's performance is compared to that of the DBN, CNN, and RNN in terms of accuracy, F-Measure, precision, recall, specificity, and sensitivity. The confusion matrix may be used to calculate the True Positive (TP), True Negative (TN), False Positive (FP), and False Negative (FN) values, which are described below:

- TP: positively predicted class as expected
- FP: unreliable positive class prediction
- FN: incorrect negative class prediction
- TN: correctly predicted negative class

Accuracy

It serves as a gauge for how well a classifier can categorize data. Equation (15) has assessed the correctness and provided the following equation.

$$\Omega_{Acc}(range\ 0-1) = \frac{TP + TN}{FP + FN + TP + TN} \quad (15)$$

Precision

Equation (16) is used to establish this definition of the relationship between the total positive results that are right and the classifier's total positive results.

$$\Omega_{\mathrm{Pre}}(range\ 0-1) = \frac{TP}{TP + FP} \quad (16)$$

Sensitivity (or recall)

Equation (17) is used to calculate it, and it relates to the TP rate of the class under consideration.

$$\Omega_{Sens}(range\ 0-1) = \frac{TP}{TP + FN} \quad (17)$$

Specificity

It relates to the TN rate of the class under consideration, or the percentage of properly detected negatives. The specificity determined by Equation (18) is given in the following equation.

$$\Omega_{Speci}(range\ 0-1) = \frac{TN}{TN + FP} \quad (18)$$

F1 score

The weighted average is derived by applying the following Equation (19), which takes into account the accuracy and recall values.

$$\Omega_{F1\_Score} = \frac{2 * TP}{FP + FN + (2 * TP)} \quad (19)$$

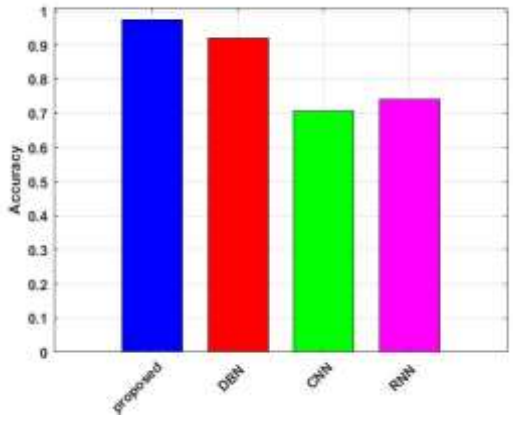

(a)

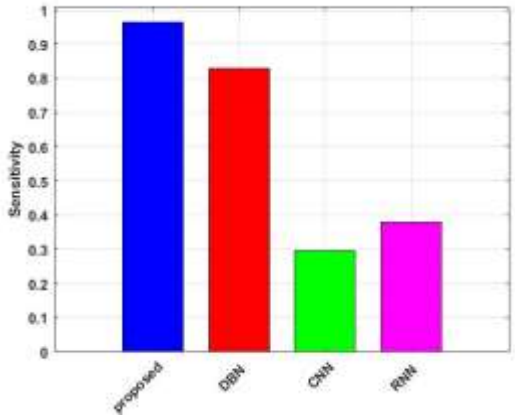

(b)

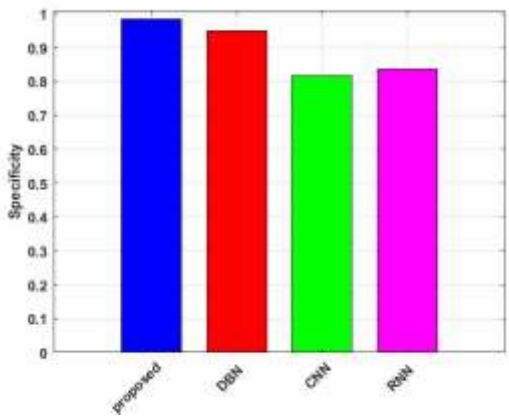

(c)

Figure 5 Comparative analysis of (a) Accuracy (b) Sensitivity and (c) Specificity

In Figure 5 shows that the comparative analysis performance metrics has been evaluated. The accuracy, sensitivity and specificity analysis of the proposed LCL-DLNN based detect the retinal disease is compared with the existing DBN, CNN and RNN approaches with respect to the accuracy, sensitivity and specificity metrics. Here, the accuracy of the proposed methodology is above 0.98 but other two methods have 0.92 for DBN, 0.7 for the CNN approach and 0.75 for the RNN approach. The sensitivity and specificity value are worst for the existing DBN, RNN when compared with the existing CNN. But the CNN also has lowest sensitivity and specificity value. Thus, it indicates that the proposed method-based detect the retinal disease better result than the existing research approaches.

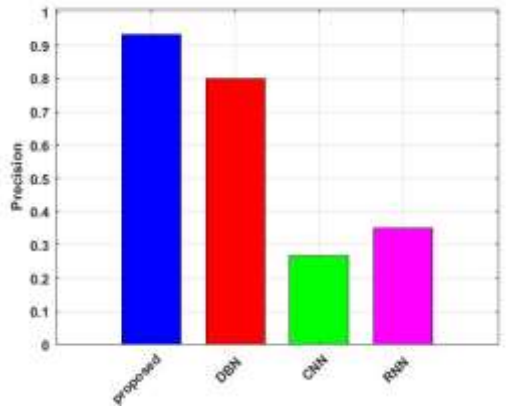

(a)

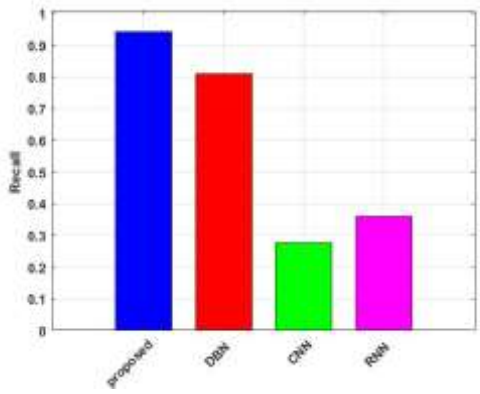

(b)

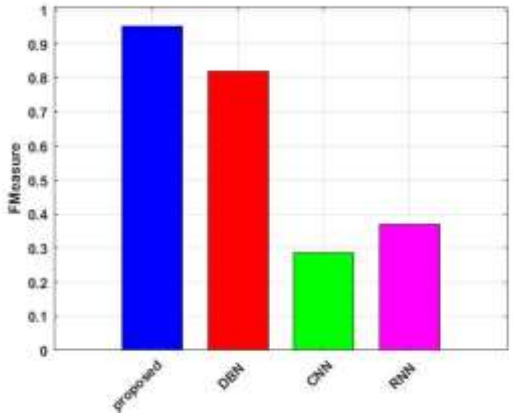

(c)

Figure 6 Comparative analysis of (a) Precision (b) Recall and (c) F-Measure

Figure 6 displays the precision, recall and F-measure analysis of the proposed and existing DBN, CNN and RNN approaches. The precision, recall and F-measure value of the proposed method is above 0.9 but the DBN, CNN and RNN attains less precision, recall and F-measure values when compared to the proposed research approach. Because the suggested study approach employs a distribution function-based output layer and a superior activation function. As a result, the graphical depiction demonstrates that the suggested technique outperforms the already used research approaches.

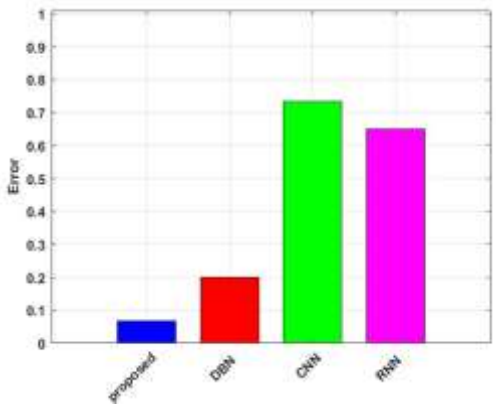

Figure 7 Comparative analysis of Error value

Figure 7 shows a comparative study of the error values of many suggested and current approaches, including DBN, CNN, and RNN. The suggested method's error value in this case is 0.075, while the high error values of the existing techniques BDN, CNN, and RNN are 0.2, 0.73, and 0.65, respectively. From the above figures, we can understand that compared to the existing DPN, CNN and RNN approach, the proposed method is better in detecting retinal disease using retinal fundus image.

V. CONCLUSION

This research proposes an effective retinal illness diagnostic method employing modern LCL-DLNN algorithm and retinal fundus image. Here, the input image is pre-processed by being cropped and the image contrast level is adjusted using ADPHE. Thesegmentation of retinal fundus image is done by the ESFIRG and the detection of retinal disease using LCL-DLNN. To create a feature vector for the final classification, the features are first extracted and then merged. Due to its enhanced performance, the proposed method can be utilised as a pre-processing tool for image segmentation, classification, and feature extraction. In an image of the retinal fundus, it may also be utilized to identify retinal diseases. In experimental analysis the performance of the proposed approach is analyzed with the existing research approaches. The proposed segmentation and prediction the proposedLCL-DLNN is compared with the existing DBN, CNN and RNN approaches. The attained accuracy, sensitivity, specificity, precision and F-measure of our proposed method are 0.98, 0.97, 0.99, 0.94and 0.95 correspondingly. The suggested study outperforms existing methods in every parameter, according to the data. In addition, as part of our continuing study, we poverty to expand the scope of the suggested method's applicability to include other types of medical imaging, such OCTA images. Other criteria may potentially be employed in addition to those mentioned in the technical research.

REFERENCES

1. Maninis, Kevis-Kokitsi, et al. "Deep retinal image understanding." Medical Image Computing and Computer-Assisted Intervention–MICCAI 2016: 19th International Conference, Athens, Greece,

October 17-21, 2016, Proceedings, Part II 19. Springer International Publishing, 2016.

2. Sim, Dawn A., et al. "Automated retinal image analysis for diabetic retinopathy in telemedicine." Current diabetes reports 15 (2015): 1-9.
3. Fu, Huazhu, et al. "Evaluation of retinal image quality assessment networks in different color-spaces." Medical Image Computing and Computer Assisted Intervention–MICCAI 2019: 22nd International Conference, Shenzhen, China, October 13–17, 2019, Proceedings, Part I 22. Springer International Publishing, 2019.
4. Xu, Xiayu, et al. "An improved arteriovenous classification method for the early diagnostics of various diseases in retinal image." Computer methods and programs in biomedicine 141 (2017): 3-9.
5. Zhou, Mei, et al. "Color retinal image enhancement based on luminosity and contrast adjustment." IEEE Transactions on Biomedical engineering 65.3 (2017): 521-527.
6. Jamal, Arshad, et al. "Retinal imaging analysis based on vessel detection." Microscopy research and technique 80.7 (2017): 799-811.
7. Sarki, Rubina, et al. "Automated detection of mild and multi-class diabetic eye diseases using deep learning." Health Information Science and Systems 8.1 (2020): 32.
8. Tufail, Adnan, et al. "Automated diabetic retinopathy image assessment software: diagnostic accuracy and cost-effectiveness compared with human graders." Ophthalmology 124.3 (2017): 343-351.
9. Colas, E., et al. "Deep learning approach for diabetic retinopathy screening." Acta Ophthalmologica 94 (2016).
10. Vujosevic, Stela, et al. "Screening for diabetic retinopathy: new perspectives and challenges." The Lancet Diabetes & Endocrinology 8.4 (2020): 337-347.
11. Imran, Azhar, et al. "Comparative analysis of vessel segmentation techniques in retinal images." IEEE Access 7 (2019): 114862-114887.
12. Mahiba, C., and A. Jayachandran. "Severity analysis of diabetic retinopathy in retinal images using hybrid structure descriptor and modified CNNs." Measurement 135 (2019): 762-767.
13. Rahim, Sarni Suhaila, et al. "Automatic screening and classification of diabetic retinopathy and maculopathy using fuzzy image processing." Brain informatics 3 (2016): 249-267.
14. Sharmila, C., and N. Shanthi. "Retinal Image Analysis for Glaucoma Detection Using Transfer Learning." Advances in Electrical and Computer Technologies: Select Proceedings of ICAECT 2020. Springer Singapore, 2021.
15. Shankar, K., et al. "Automated detection and classification of fundus diabetic retinopathy images using synergic deep learning model." Pattern Recognition Letters 133 (2020): 210-216.
16. Butt, Muhammad Mohsin, et al. "Diabetic Retinopathy Detection from Fundus Images of the Eye Using Hybrid Deep Learning Features." Diagnostics 12.7 (2022): 1607.
17. Gampala, Veerraju, et al. "Glaucoma detection using hybrid architecture based on optimal deep neuro fuzzy network." International Journal of Intelligent Systems 37.9 (2022): 6305-6330.
18. Muthukannan, P. "Optimized convolution neural network based multiple eye disease detection." Computers in Biology and Medicine 146 (2022): 105648.
19. Ramya, J., M. P. Rajakumar, and B. Uma Maheswari. "Deep CNN with hybrid binary local search and particle swarm optimizer for exudates classification from fundus images." Journal of Digital Imaging 35.1 (2022): 56-67.
20. Kadry, Seifedine, et al. "Automated detection of age-related macular degeneration using a pre-trained deep-learning scheme." The Journal of Supercomputing (2022): 1-20.
21. Singh, Law Kumar, et al. "Collaboration of features optimization techniques for the effective diagnosis of glaucoma in retinal

fundus images." Advances in Engineering Software 173 (2022): 103283.

22. Khaing, Tin Tin, et al. "Vessel-based hybrid optic disk segmentation applied to mobile phone camera retinal images." Medical & Biological Engineering & Computing (2022): 1-17.
23. Kandhway, Pankaj, Ashish Kumar Bhandari, and Anurag Singh. "A novel reformed histogram equalization based medical image contrast enhancement using krill herd optimization." Biomedical Signal Processing and Control 56 (2020): 101677.
24. Chen, Hongwei, et al. "Evaluation on diabetic plantar pressure data-set employing auto-segmentation technologies." Neural Computing and Applications 32 (2020): 11041-11054.
25. Fang, Jiangxiong, Huaxiang Liu, Liting Zhang, Jun Liu, and HeshengLiu.. "Region-edge-based active contours driven by hybrid and local fuzzy region-based energy for image segmentation." Information Sciences 546 (2021): 397-419.
26. Shoukat, Ayesha, and Shahzad Akbar. "Artificial intelligence techniques for glaucoma detection through retinal images: State of the art." Artificial Intelligence and Internet of Things (2021): 209-240.
27. Bodapati, Jyostna Devi, Nagur Shareef Shaik, and VeeranjaneyuluNaralasetti. "Deep convolution feature aggregation: an application to diabetic retinopathy severity level prediction." Signal, Image and Video Processing 15 (2021): 923-930.
28. Saranya, P., et al. "Blood vessel segmentation in retinal fundus images for proliferative diabetic retinopathy screening using deep learning." The Visual Computer (2022): 1-16.
29. Benítez, Veronica Elisa Castillo, et al. "Dataset from fundus images for the study of diabetic retinopathy." Data in brief 36 (2021): 107068.